Optics Communications 283 (2010) 3520–3524

Contents lists available at ScienceDirect

Optics Communications

journal homepage: www.elsevier.com/locate/optcom

Enhancement of terahertz wave difference frequency generation based on a compact walk-off compensated KTP OPO

Kai Zhong [a,b,*], Jianquan Yao [a,b], Degang Xu [a,b], Zhuo Wang [a,b], Zhongyang Li [a,b], Huiyun Zhang [a,c], Peng Wang [a,b]

[a] Institute of Laser and Optoelectronics, College of Precision Instrument and Optoelectronics Engineering, Tianjin University, Tianjin 300072, China
[b] Key Laboratory of Optoelectronic Information Science and Technology, Ministry of Education, Tianjin University, Tianjin 300072, China
[c] College of Science, Shandong University of Science and Technology, Qingdao 266510, China

ARTICLE INFO

Article history:
Received 25 February 2010
Received in revised form 29 April 2010
Accepted 30 April 2010

Keywords:
Terahertz wave
Difference frequency generation
Walk-off compensate
GaSe

ABSTRACT

A compact, walk-off compensated dual-wavelength KTP OPO near the degenerate point of 2.128 μm pumped by a Nd:YAG pulsed laser is employed as the pump for terahertz (THz) source based on difference frequency generation (DFG) in a GaSe crystal. Coherent THz radiation that is continuously tunable in the range of 81–1617 μm (0.186–3.7 THz) is achieved. An enhancement of 76.7% in average for the THz energies at different wavelengths is realized using the walk-off compensated KTP OPO than the common one. Using a 8 mm-long GaSe crystal, the maximum output THz pulse energy is 48.9 nJ with the peak power of 11 W, corresponding to the energy conversion efficiency of 5.4×10^{-6} and the photon conversion efficiency of about 0.09%.

1. Introduction

Compact, efficient, widely-tunable coherent terahertz (THz) sources provide us convenient facilities in frequency domain spectroscopy and imaging. To satisfy such requirements, various methods have been exploited based on difference frequency generation (DFG) using nonlinear crystals such as $LiNbO_3$ [1], PPLN [2], GaP [3], GaSe [4], $ZnGeP_2$ [5], GaAs [6], DAST [7], and so on. The generated peak powers for nanosecond THz pulses have exceeded 2 kW [6], and even reached the order of MW for picosecond short pulses [8]. However, most of the reported DFG systems are very bulky and complicated, restricted by the dual-wavelength-laser generating methods employing huge dye [1], CO_2 [6,8], or solid-state lasers and optical parametric oscillators (OPOs), optical splitters/combiners, time delay systems, wave-plates etc. Portable coherent terahertz sources are still urgently needed for practical applications.

Among the DFG crystals mentioned above, GaSe has the lowest absorption coefficients in the THz wavelength region, and it is transparent in the near infrared region around 1 μm. GaSe has a large second-order nonlinear coefficient (54 pm/V) and its large birefringence allows phase-matching in an ultra-broad wavelength range. Shi et al. have reported THz generation of 0.18–5.27 THz based on DFG in GaSe [4], and the maximum THz peak power reaches 389 W using a 47 mm-long GaSe crystal [9]. As a mid-infrared nonlinear crystal, the absorption of GaSe in THz region cannot be ignored, as this parameter plays a key role in THz generation. Merely increasing the length of crystal may even counter-affect the conversion efficiency when there is obvious absorption. Several points should be considered when designing the DFG system in order to obtain higher THz output energy. Firstly, the crystal length should be optimized for certain absorption coefficients; secondly, the pump laser must be well-designed and dual-wavelength laser pulses with better beam quality should be employed; thirdly, the injected intensity should be appropriate under the permission of the damage threshold for a certain DFG crystal, which means we have to balance the contradiction between using higher pump intensity to enhance conversion efficiency and preventing the back conversion from THz to pump wavelength with excessively high pump intensity. Besides, using pump laser with longer wavelength will proportionally increase the quantum efficiency according to the Manley–Rowe relations, but such pump lasers with narrow line widths are difficult to achieve except the discontinuously tunable bulky CO_2 lasers [6,8].

The DFG process in GaSe crystal is theoretically analyzed in this paper, and in the experiment we introduce a walk-off compensated intracavity pumped dual-wavelength KTP OPO into THz DFG system for the first time. The KTP OPO is doubly resonant and works near the degenerate point at 2.128 μm, which doubles the quantum efficiency compared with DFG using pump pulses around 1 μm. Besides lower threshold and better stability, the walk-off compensated KTP OPO greatly improves the pump beam quality and enhances the DFG conversion efficiency. This THz source is simple and compact, about

* Corresponding author. Institute of Laser and Optoelectronics, College of Precision Instrument and Optoelectronics Engineering, Tianjin University, Tianjin 300072, China. Tel.: +86 22 27407676; fax: +86 22 27406436.
E-mail address: zhongkai1984@gmail.com (K. Zhong).

0030-4018/$ – see front matter © 2010 Elsevier B.V. All rights reserved.
doi:10.1016/j.optcom.2010.04.106

$10\times10\times40\ \mathrm{cm}^2$ in size, therefore it provide us a novel method for portable THz systems. The generated THz tuning range is from 0.186 THz to 3.7 THz with the maximum peak power of 11 W at 1.68 THz. An average enhancement of 76.7% for the THz energies is realized using the walk-off compensated KTP OPO than the common one.

2. Theoretical analysis of DFG in GaSe with absorption

During the DFG process, the applied waves with frequencies ω_1 and ω_2 interact with each other in the nonlinear optical medium to generate a new wave at terahertz frequency ω_T ($\omega_1-\omega_2=\omega_T$). Taking absorption into account, this interaction is described by the one-dimensional coupled-wave equations propagating along the z-direction [10]

$$\frac{dA_1}{dz} = -\frac{\alpha_1}{2}A_1 - \frac{i\omega_1 d_{\mathrm{eff}}}{cn_1}A_2A_T e^{i\Delta kz} \tag{1.1}$$

$$\frac{dA_2}{dz} = -\frac{\alpha_2}{2}A_2 - \frac{i\omega_2 d_{\mathrm{eff}}}{cn_2}A_1A_T^* e^{-i\Delta kz} \tag{1.2}$$

$$\frac{dA_T}{dz} = -\frac{\alpha_T}{2}A_T - \frac{i\omega_T d_{\mathrm{eff}}}{cn_T}A_1A_2^* e^{-i\Delta kz} \tag{1.3}$$

where A_1, A_2, A_T are the complex electric field of the three waves in the nonlinear crystal, d_{eff} is the effective nonlinear coefficient, α_1, α_2, α_T are the attenuation coefficients in the nonlinear crystal, n_1, n_2, n_T are the refractive indices, c is the speed of light, and $\Delta k=k_1-k_2-k_3$ is the phase-mismatching.

The intensities of the three waves are expressed as $I_{1,2,T}=1/2\varepsilon_0 cn_{1,2,T}|A_{1,2,T}|^2$, where ε_0 is the vacuum permittivity. Taking a KTP OPO operating near the degenerate point of 2.128 μm for example and assuming two pump waves with the wavelengths of 2.116 μm and 2.141 μm interact in a GaSe crystal, the generated THz wavelength is 181 μm (or 1.66THz in frequency). If all the absorptions in the crystal are ignored, the calculated intensities of the three waves are shown in Fig. 1. The parameters in the calculation are $\varepsilon_0=8.854$ pF/m, $d_{\mathrm{eff}}=54$ pm/V, $c=3\times10^8$ m/s, $n_1=2.7437$, $n_2=2.4146$, $n_T=3.2889$, $\Delta k=0$ and the initial condition of pump intensity for each wave is 10 MW/cm^2, which is lower than the damage threshold of GaSe for the total.

It is obvious that the intensities of the generated THz wave and one of the pump waves at lower frequency increases with the propagation length in GaSe crystal. The reason is that each photon at frequency ω_1 participating in this process is converted into two photons at frequency ω_2 and terahertz frequency ω_T. It is appreciated that the input pump intensity at higher frequency is higher than that the other one, however, equivalent energy are used here because the two pump waves are generated simultaneously in our scheme. Cronin-Golomb has analyzed cascaded DFG in ZnTe [11] which can greatly increase the conversion efficiency to THz wave and even overcome Manley–Rowe limit, but such phenomenon is restrained by the phase-matching condition based on birefringence and the low damage threshold of GaSe.

As a matter of fact, almost all the nonlinear materials have relatively high absorption coefficients in THz region, which greatly affects the DFG efficiency. Fig. 2 depicts the variety of THz intensities with different absorption coefficients. It is supposed that the absorption coefficient around 2 μm in GaSe is 0.1 cm^{-1} and all the other parameters are the same as that mentioned above. With certain absorption coefficients α_T, the maximum output THz intensities reduce distinctly and there is an optimized crystal length l_0 for each α_T. Using a nonlinear crystal that is longer than l_0 the conversion efficiency will be depressed. l_0 equal to 31.4 mm, 23.7 mm, 18.7 mm and 13.3 mm when $\alpha_T=1$ cm^{-1}, 2 cm^{-1}, 3 cm^{-1}, and 5 cm^{-1} respectively, presenting a shortening tendency with the increase of absorption coefficient.

Fig. 3 shows the relation of generated THz intensity to the pump intensity (1–15 MW/cm^2) and wavelength (50–3000 μm). A 10 mm-long GaSe crystal is taken for example and the THz absorption coefficient is 3 cm^{-1} in calculation. We can see that extremely high THz intensity can be achieved at the low wavelength end with pump intensity that is high enough. However, the deviation between theoretical and experiment results can be quite large. This is because not only the THz absorption leaps significantly at short THz wavelength, but also the increase of Fresnel reflection with the phase-matching angle, which will be illustrated in the fourth part of the text.

3. Experimental setup

The schematic of the terahertz source based on DFG in GaSe is shown in Fig. 4. The dual-wavelength KTP OPO is intracavity pumped by a diode-side-pumped electro-optic Q-switched Nd:YAG laser and works near the degenerate point of 2.128 μm with the repetition rate of 10 Hz. The Nd:YAG rod is 115 mm in length and 5 mm in diameter. A diaphragm (D) with a diameter of 3 mm is inserted to the laser cavity to reduce spot size instead of using focusing lenses behind the OPO cavity. M_1 and M_3 form a plane-parallel laser cavity at 1.06 μm

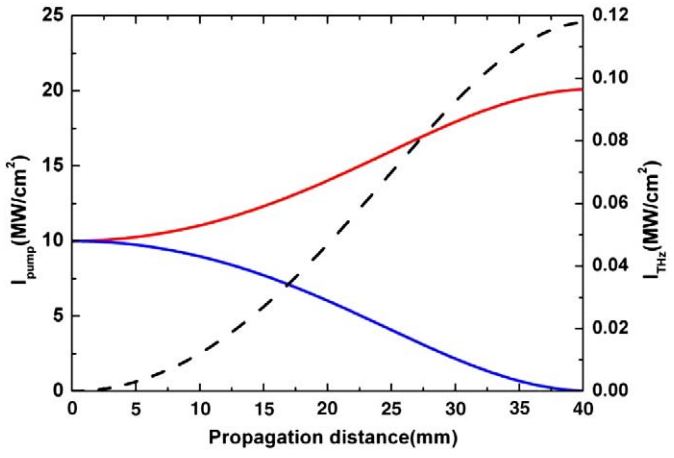

Fig. 1. The three-wave intensity variation with the propagation distance in GaSe if the absorptions are ignored. The solid curves are the two pump waves (ω_1—the lower one, ω_2—the upper one) and the dashed line is the THz wave.

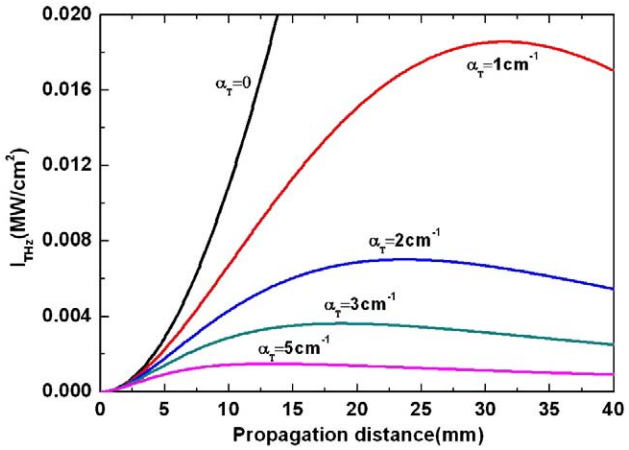

Fig. 2. Generated THz intensity using different GaSe crystals with different absorption coefficients.

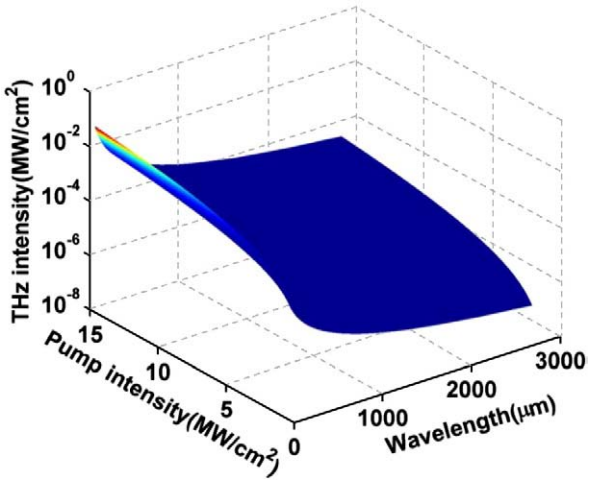

Fig. 3. Generated THz intensity versus the pump intensity and THz wavelength with a 10 mm-long and $\alpha_T = 3\ cm^{-1}$ GaSe crystal.

and they are both highly-reflective (HR) coated at 1.06 μm. M_3 also has a transmission of 50% at 1.9–2.4 μm as one of the OPO cavity mirror. M_2 is anti-reflective (AR) coated at 1.06 μm and HR coated at 1.9–2.42 μm, constructing a doubly resonant OPO cavity with M_3. The KTP crystals are $7\times8\times15\ mm^3$, uncoated and cut at $\theta = 49.5°$, $\varphi = 0°$, which are tuned in the a–c plane to achieve type-II ($o \rightarrow e + o$) phase-matching. The total laser cavity length from M_1 to M_3 is 350 mm and the OPO cavity length is 55 mm. A dichroic mirror (DM) coated for HR at 1.06 μm and AR at 1.8–2.5 μm is used to filter out the fundamental wave before the dual-wavelength laser pulses are injected into the nonlinear crystal directly. We use a commercial GaSe crystal which is 8 mm-long and uncoated at both faces for DFG. The generated THz wave is detected with a 4 K Si-bolometer after focusing with a white polyethylene lens (L) and filtered by a germanium wafer coated for HR at 1.8–2.5 μm.

The KTP OPO consists of one or two identical uncoated KTP crystals. For the former arrangement, the walk-off limits the beam overlap of the output signal and idler waves, which is a concern for DFG, particularly for small diameter beams. In the case with two KTP crystals, they are arranged in a configuration that the KTP2 has a π rotation by KTP1 around the x-axis of the laboratory frame defined by the propagating directions. The walk-off between the wave vector and energy flow for the e-wave in KTP1 is compensated by the other one while keeping the sign of d_{eff} in KTP2 unchanged in this configuration [12]. The spatial separation of the two output beam is eliminated and the single-pass parametric gain is doubled ignoring the reflections at the ends of KTP crystals, both of which improve the total conversion efficiency. There is also another advantage that the oscillating threshold can be reduced because the parametric process in the second crystal is seeded by the signal (idler) waves generated in the first one.

4. Experimental results and discussions

The pump beam of the KTP OPO was linearly polarized along the b-axis (o-ray), while the generated signal and idler waves are linearly polarized along the b-axis (o-ray) or in the a–c plane (e-ray), respectively. Here a, b and c are the principle axes of the index ellipsoid ($n_a < n_b < n_c$). Tuned from 46.7° to 52.8° for the internal phase-matching angle in the a–c plane, the wavelength range from 1.82 μm to 2.56 μm is covered, as shown in Fig. 5. The wavelengths are monitored by an Agilent 86142B spectrometer (measuring range 600–1700 nm) through the frequency-doubled waves using another KTP crystal (cut at $\theta = 50.5°$, $\varphi = 0°$, $7\times7\times7\ mm^3$ in size). The second harmonic wave of the KTP OPO has a pulse-width of about 4.5 ns and

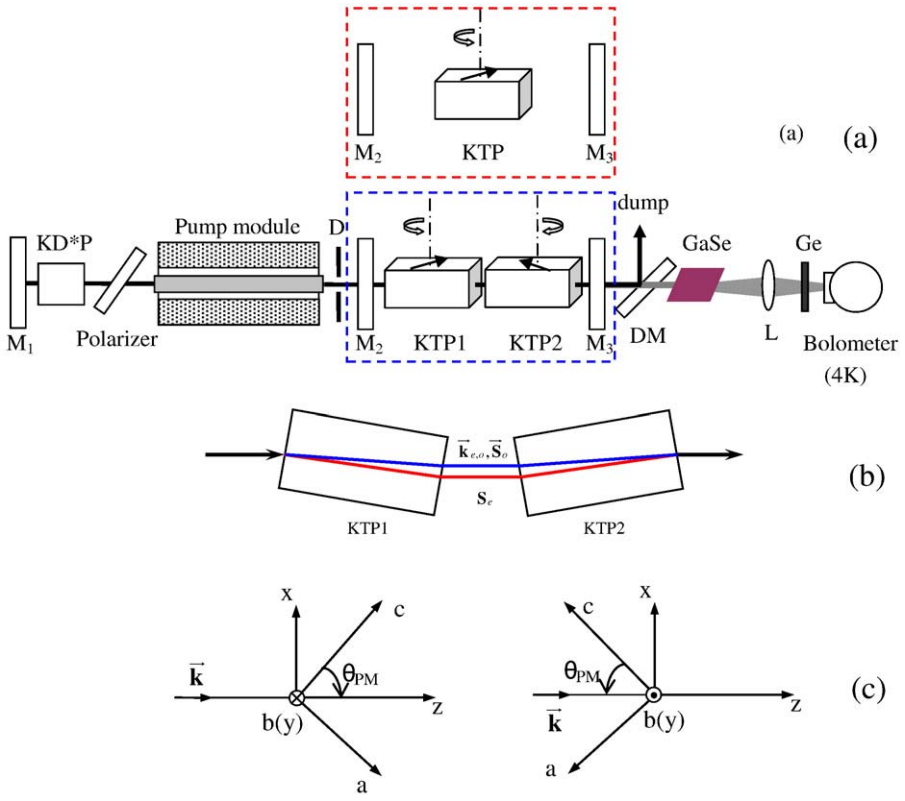

Fig. 4. Experimental setup of the THz source: (a), schemes of dual-wavelength KTP OPO (the fundamental-wave polarization is parallel to the tuning plane) with one (in the red frame) or two KTPs (in the blue frame); (b) and (c), the twin-crystal walk-off compensated arrangement (vertical view of (a)).

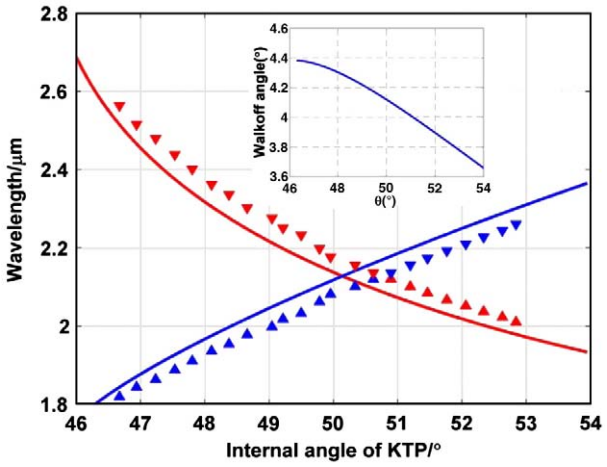

Fig. 5. Angle tuning characteristics of the KTP OPO and the corresponding walk-off angles. The triangles and the solid curve represent the experimental and theoretical results (calculated with Sellmeier equations in [13]).

linewidth of around 1 nm. To avoid optical damage to the GaSe crystal, the input dual-wavelength energy was restricted to 9 mJ during the experiment.

The walk-off angle for signal wave is around 4°, which means the maximum spatial separation is about 1 mm after single-pass propagation in a 15 mm-long KTP crystal. With the walk-off compensated scheme, the walk-off direction is reversed in the second crystal and the counteraction compensates the spatial divergence. Not only the beam quality, but also the operating characteristics are improved. The threshold pump current is reduced by 2 amperes (the pump peak power of the LD arrays is reduced by 25%) with higher gain and the output instability (rms) at 9 mJ is reduced from 9.35% to 6.6% in the experiment.

Type o–e→e (oee) DFG can be phase-matched in a GaSe crystal pumped by a near-degenerate dual-wavelength KTP OPO around 2.13 μm. As the effective nonlinear optical coefficient that is dependent on the phase-matching and azimuthal angle is $d_{\text{eff}} = d_{22}\cos 2\theta \cos 3\varphi$, the GaSe crystal is rotated around the x-axis ($\varphi = 0$) of the crystal so that $\cos 3\varphi = 1$ can be assured in the experiment. Fig. 6 shows the phase-matching tuning curves with external angle. Tunable and coherent THz radiation from 81 μm to 1617 μm (0.186–3.7THz) is achieved when the two pump waves are in the range of 2.101–2.1272 μm (o-wave) and 2.157–2.13 μm (e-wave), respectively. The long-wavelength cutoff is limited by the sensitivity of the detector because the THz signal decreases as the wavelength increases. The short-wavelength end, however, is limited by the rapidly increased absorption coefficient of the GaSe crystal and the depressed conversion efficiency with the increase of phase-matching angle.

Fig. 7 shows the measured THz wave output energy versus frequency. With the walk-off compensated scheme and considering the transmittance of the focusing lens, germanium filter and THz attenuators (Microtech Instruments Inc.) used to prevent saturation of the bolometer, the maximum output energy is 48.9nJ (about 1.54×10^{-4} MW/cm^2 in intensity at the output face of the GaSe crystal) at the frequency of 1.68THz (178.7 μm in wavelength), corresponding to the energy conversion efficiency of 5.4×10^{-6} or photon conversion of about 0.09%. The maximum peak power is about 11 W referring to the pulse-width of the pump wavelength. The THz energy at 0.186 THz and 3.7 THz is 0.39 nJ and 0.29nJ, respectively. The sharp decline at about 3THz is caused by the transmission cutoff around 100 μm for the filter inside the bolometer (the actual energy above 3 THz should be much higher). According to the absorption coefficient curve of our GaSe crystal measured with a terahertz time domain system, which is shown in Fig. 8, the maximum energy is obtained at the window with relatively low absorption in GaSe, which is above 3 cm^{-1} all the same. The output THz pulse energy should be much higher with a better DFG crystal.

The output THz intensity under phase-matching conditions can be obtained from solving the coupling wave equations [4]

$$I_T = \frac{1}{2}\left(\frac{\mu_0}{\varepsilon_0}\right)^{3/2}\frac{\omega_T^2 d_{\text{eff}}^2 L^2}{n_1 n_2 n_3} I_1 I_2 T_1 T_2 T_T \exp(-\alpha_1 L)\left[\frac{1-\exp(-\Delta\alpha L)}{-\Delta\alpha L}\right]^2. \quad (2)$$

Here $T_{1,2,T}$ are the Fresnel transmission coefficients for the three waves at each facet and they increase with the phase-matching angle at the short THz wavelength end. From Fig. 7 we can see that employing the walk-off compensated KTP OPO with the energy of higher pump intensity at 9 mJ and using a longer GaSe crystal of 8 mm, the total THz energy is increased almost exponentially according with Eq. (2). All the results are repeatable in experiment. An enhancement of about 76.7% in average is achieved using the walk-off compensated KTP OPO, which confirms the advantages of the dual-wavelength pump laser with the improved scheme.

The divergence half-angle of the generated THz beam at maximum energy is about 90 mrad, measured with a knife edge. It should also be noted that the conversion efficiency is still quite low. That is because

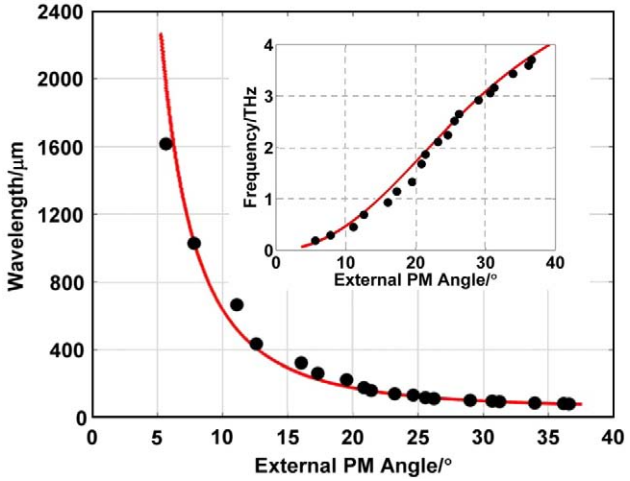

Fig. 6. THz tuning characteristics with the PM angles. Circles and the solid curve represent the experimental and theoretical results (calculated with Sellmeier equations in [14]).

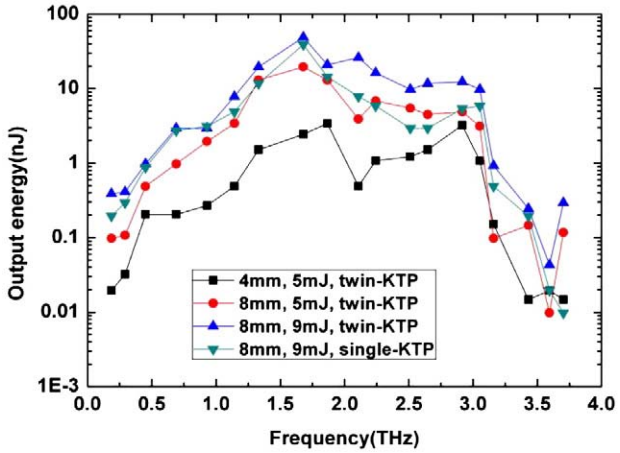

Fig. 7. Output THz pulse energy versus THz frequency with different pump energies, nonlinear crystals, and OPO schemes.

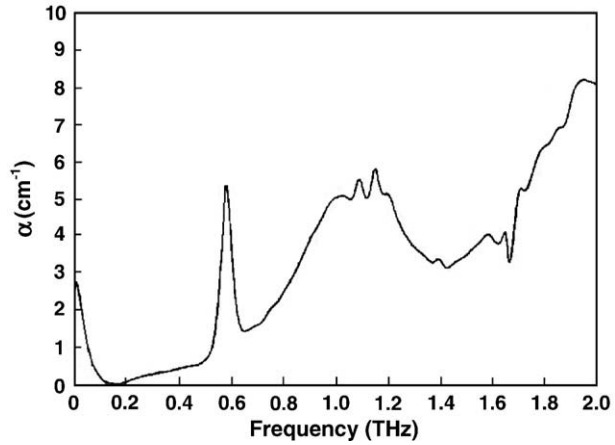

Fig. 8. Absorption coefficient for the 8 mm-long GaSe crystal in the experiment.

the short crystal length, dissatisfying crystal quality and the relatively low pump density without any focusing in our experiment, compared with Refs. [4,8]. It is believed that the conversion efficiency will be increased remarkably if these conditions are improved.

5. Conclusion

A compact coherent THz source that is continuously tunable in the range of 81–1617 μm (0.186–3.7THz) based on DFG in a 8 mm-long GaSe crystal has been demonstrated. Using a simple walk-off compensated dual-wavelength KTP OPO as the pump source, we achieve THz output single pulse energy of 48.9nJ with the peak power of 11 W, corresponding to the energy conversion efficiency of 5.4×10^{-6} and the photon conversion efficiency of about 0.09%. Besides the improvement in the pump threshold, conversion efficiency and operating stability of the KTP OPO, the generated THz energy is increased by 76.7% with the walk-off compensated scheme. There is still much space to better the output THz energy and conversion efficiency according to our theoretical analysis.

Acknowledgments

This work is supported by the National Basic Research Program of China under Grant No. 2007CB310403, the Research Fund for the Doctoral Program of Higher Education under Grant No. 20070420118, the National Natural Science Foundation of China under Grant No. 60801017 and No. 10874128.

References

[1] K.H. Yang, J.R. Morris, P.L. Richards, Y.R. Shen, Appl. Phys. Lett. 23 (1973) 669.
[2] Y. Sasaki, A. Yuri, K. Kawase, H. Ito, Appl. Phys. Lett. 81 (2002) 3323.
[3] T. Tanabe, K. Suto, J. Nishizawa, K. Saito, T. Kimura, Appl. Phys. Lett. 83 (2003) 237.
[4] W. Shi, Y.J. Ding, N. Fernelius, K. Vodopyanov, Opt. Lett. 27 (2002) 1454.
[5] W. Shi, Y.J. Ding, Appl. Phys. Lett. 83 (2003) 848.
[6] S.Ya. Tochitsky, C. Sung, S.E. Trubnick, C. Joshi, K.L. Vodopyanov, J. Opt. Soc. Am. B 24 (2007) 2509.
[7] T. Taniuchi, J. Shikata, H. Ito, Electron. Lett. 36 (2000) 1414.
[8] S.Ya. Tochitsky, J.E. Ralph, C. Sung, C. Joshi, J. Appl. Phys. 98 (2005) 026101.
[9] W. Shi, Y.J. Ding, Int. J. High Speed Electron. Syst. 16 (2006) 589.
[10] A. Yariv, Quantum Electronics, Wiley, New York, 1988.
[11] M. Cronin-Golomb, Opt. Lett. 29 (2004) 2046.
[12] D.J. Armstrong, W.J. Alford, T.D. Raymond, A.V. Smith, J. Opt. Soc. Am. B 14 (1997) 460.
[13] K. Kato, E. Takaoka, Appl. Opt. 41 (2002) 5040.
[14] K.L. Vodopyanov, L.A. Kulevskii, Opt. Commun. 118 (1995) 375.